A Weak Calcium Binding Site in Subtilisin BPN′ Has a Dramatic Effect on Protein Stability

Richard D. Kidd,[†] Hemant P. Yennawar,[†] Pamela Sears,[‡] Chi-Huey Wong,[‡] and Gregory K. Farber*[,†]

Contribution from the Department of Biochemistry and Molecular Biology, Center for Biomolecular Structure and Function, The Pennsylvania State University, 108 Althouse Laboratory, University Park, Pennsylvania 16802, and Department of Chemistry, The Scripps Research Institute, 10666 North Torrey Pines Road, La Jolla, California 92037

Received October 12, 1995[⊗]

Abstract: The crystal structures of both subtilisin 8397 and a thermostable variant (Lys 256 Tyr) have been determined to 2.2 and 1.8 Å resolution. The thermostable variant (8397+1) was previously shown to exhibit enhanced thermostability over 8397 in both aqueous solutions and the polar organic solvent dimethylformamide (Sears, P.; *et al*. *J. Am. Chem. Soc*. **1994**, *116*, 6521−6530). The single substitution did not induce major changes in the protein structure (total rms deviation is 0.41 Å); however, changes in calcium binding were detected. The strong calcium binding site was occupied in both structures as has been seen in other subtilisins (Pantoliano, M.; *et al*. *Biochemistry* **1988**, *27*, 8311−8317). Unexpectedly, the weak calcium binding site was occupied in the 8397+1 structure but not in the 8397 structure. The goal of the Lys 256 Tyr mutation was to improve the stability of subtilisin in DMF by removing a surface charge. However, changing this residue altered calcium binding at a site 12 Å away, illustrating the importance of structure determination in understanding stability changes.

Introduction

Subtilisin BPN′ (EC 3.4.21.14), a serine protease from *Bacillus amyloliquefaciens*, has received a great deal of attention as a catalyst for peptide synthesis.[1,2] Current solid-phase peptide syntheses require extensive protection and deprotection steps and suffers from racemization and low solubility of many derivatized amino acids and peptides in common solvents. The use of a serine protease like subtilisin to catalyze peptide bond formation would be ideal for reducing the need for protecting groups and for nearly eliminating the problem of racemization.[3] *N*,*N*-Dimethylformamide (DMF) is useful for both solubilizing amino acids and for shifting the equilibrium away from proteolysis and toward peptide synthesis by reducing the availability of water.[4] Unfortunately, wild-type subtilisin has a half-life of only 20 min in anhydrous DMF compared to 15 h in aqueous solution.[5] In order to increase the stability of subtilisin in DMF, site-directed mutagenesis has been used to create a series of mutants.[5−8] Several of these mutants showed dramatic increases in half-life both in anhydrous DMF and in aqueous solution.[5,8]

Calcium ions have been shown to play an important role in stabilizing subtilisin by binding at specific sites. Pantoliano and co-workers[9] have previously reported high-resolution structural evidence for two calcium binding sites. One of these sites, the A site, binds Ca^{2+} with high affinity ($K_d \approx 1 \times 10^{-8}$ M).[6] The second site (B) is a weak Ca^{2+} binding site with a binding affinity of 32 mM.[9] Cations other than calcium are also known to bind at the B site which is 32 Å away from the A site.[9−11] Binding a cation in the B site dramatically improves the stability of subtilisin.[9,12]

Two mutants of subtilisin that showed marked improvements in stability have been studied in our laboratories. One of these mutants, coined 8397, was derived from subtilisin BPN′ by making five mutations.[5] The other mutant, which we have named 8397+1, has a single extra amino acid substitution (Lys 256 Tyr) compared to 8397 and is more stable in both aqueous and DMF environments than 8397.[8]

In this paper, we report the structural basis of this increased stability in an aqueous environment. In order to understand the change in stability in DMF, crystal structures in this polar solvent need to be determined. Fortunately, techniques have recently been reported to solve crystal structures of proteins in nonaqueous solvents. These structures include γ-chymotrypsin crystals in hexane[13] and 2-propanol[14] and glutaraldehyde cross-linked crystals of subtilisin Carlsberg in acetonitrile.[15] We have solved the crystal structure of subtilisin 8397+1 in a series of

* Author to whom correspondence should be addressed at the above postal address or by e-mail to farber@retina.chem.psu.edu.
† The Pennsylvania State University.
‡ The Scripps Research Institute.
⊗ Abstract published in *Advance ACS Abstracts,* February 1, 1996.

(1) Wong, C.-H. *Science* **1989**, *244*, 1145−1152.
(2) Abrahmsén, L.; Tom, J.; Burnier, J.; Butcher, K. A.; Kossiakoff, A.; Wells, J. A. *Biochemistry* **1991**, *30*, 4151−4159.
(3) Wells, J. A.; Estell, D. A. *TIBS* **1988**, *13*, 291−297.
(4) Homandberg, G. A.; Mattis, J. A.; Laskowski, M., Jr. *Biochemistry* **1978**, *17*, 5220−5227.
(5) Zhong, Z.; Liu, J. L.-C.; Dinterman, L. M.; Finkelman, M. A. J.; Mueller, W. T.; Rollence, M. L.; Whitlow, M.; Wong, C.-H. *J. Am. Chem. Soc*. **1991**, *113*, 683−684.
(6) Pantoliano, M. W.; Whitlow, M.; Wood, J. F.; Dodd, S. W.; Hardman, K. D.; Rollence, M. L.; Bryan, P. N. *Biochemistry* **1989**, *28*, 7205−7213.
(7) Wong, C.-H.; Chen, S.-T.; Hennen, W. J.; Bibbs, J. A.; Wang, Y.-F.; Liu, J. L.-C.; Pantoliano, M. W.; Whitlow, M.; Bryan, P. N. *J. Am. Chem. Soc*. **1990**, *112*, 945−953.
(8) Sears, P.; Schuster, M.; Wang, P.; Witte, K.; Wong, C.-H. *J. Am. Chem. Soc*. **1994**, *116*, 6521−6530.
(9) Pantoliano, M. W.; Whitlow, M.; Wood, J. F.; Rollence, M. L.; Finzel, B. C.; Gilliland, G. L.; Poulos, T. L.; Bryan, P. N. *Biochemistry* **1988**, *27*, 8311−8317.
(10) Kossiakoff, A. A.; Ultsch, M.; White, S.; Eigenbrot, C. *Biochemistry* **1991**, *30*, 1211−1221.
(11) Drenth, J.; Hol, W. G. J.; Jansonius, J. N.; Koekoek, R. *Eur. J. Biochem*. **1972**, *26*, 177−181.
(12) Bryan, P. N. *Biotechnol. Adv.* **1987**, *5*, 221−234.
(13) Yennawar, N. H.; Yennawar, H. P.; Farber, G. K. *Biochemistry* **1994**, *33*, 7326−7336.
(14) Yennawar, H. P.; Yennawar, N. H.; Farber, G. K. *J. Am. Chem. Soc*. **1995**, *117*, 577−585.
(15) Fitzpatrick, P. A.; Steinmetz, A. C. U.; Ringe, D.; Klibanov, A. M. *Proc. Natl. Acad. Sci. U.S.A.* **1993**, *90*, 8653−8657.

0002-7863/96/1518-1645$12.00/0

different dimethylformamide concentrations. These structures explain the lower activity of subtilisin in DMF and will be reported elsewhere. Here we report the refined crystal structures of subtilisin 8397 at 2.2 Å and subtilisin 8397+1 at 1.8 Å in aqueous solution. This pair of structures explains the increased stability of the 8397+1 mutant.

Experimental Section

Site-Directed Mutagenesis. The subtilisin-deficient *B. subtilis* strain 4935 and the subtilisin 8397-containing shuttle vector pGX5097 were obtained from the Genex Corporation. The 8397 variant contained the following amino acid substitutions compared to subtilisin BPN′:[6] Asn 218 Ser, Gln 206 Cys, Gly 169 Ala, Asn 76 Asp, and Met 50 Phe. Site-directed mutagenesis of 8397 to produce 8397+1 was performed as previously described.[8] Subtilisin 8397+1 has a additional Lys 256 Tyr substitution.

Isolation of Subtilisin Mutants. Both subtilisin 8397 and 8397+1 were isolated by the procedure of Carter and Wells,[16] with modifications. In brief, *B. subtilis* carrying the subtilisin 8397- or 8397+1-bearing plasmid pGX5097 was grown in AM3 medium (Difco) + 15 μg/mL kanamycin for 2 days. The cells were removed by centrifugation, and the supernatant was precipitated with first 40% and then 70% ammonium sulfate. The precipitant from the 40−70% cut was dialyzed against distilled water. After dialysis, MES/$CaCl_2$ (pH 6.0) was added at a 1:10 ratio to give a final concentration of 10 mM MES/5 mM $CaCl_2$. The subtilisin was run through DEAE cellulose (DE-52, Whatman) equilibrated with 10 mM MES/5 mM $CaCl_2$. As an additional step for crystallography, the protein was run through a carboxymethylcellulose column (CM-52, Whatman), pre-equilibrated with 10 mM MES/5 mM $CaCl_2$ (pH 6.0), and eluted with a 10 mM MES/5 mM $CaCl_2$ (pH 6.0) to 100 mM MES/50 mM $CaCl_2$ (pH 6.0) linear gradient. Column fractions were monitored using activity measurements with succinyl-Ala-Ala-Pro-Phe-*p*-nitroanilide as the substrate.[8] Active fractions were pooled, dialyzed against 4 × 4 L of distilled water, and then lyophilized to dryness.

Crystal Preparation. Subtilisin (either 8397 or 8397+1) was dissolved at 10 mg/mL in 10 mM sodium cacodylate (pH 4.6) and then dialyzed overnight against this buffer at 4 °C. For preliminary crystallization trials, a sparse matrix screen (Hampton Research) was employed. This screen was developed by Jancarik and Kim[17] following the earlier suggestions of Carter and Carter.[18] Crystals of subtilisin 8397+1 were initially obtained as twinned rods (100 × 20 × 20 μm) in 20% (v/v) 2-propanol, 100 mM sodium citrate (pH 5.6), and 20% (w/v) PEG 3400. The concentrations of 2-propanol and PEG 3400 were both varied in a two-dimensional grid to optimize the quality of these crystals. Similar optimization experiments with subtilisin 8397 failed to improve crystal quality.

For data collection, subtilisin 8397 was crystallized by hanging drop vapor diffusion in 24-well tissue culture plates (Falcon). The coverslips used were coated with Sigmacote prior to crystallization attempts. The initial protein drop (20 μL) contained 5 mg/mL protein, 5 mM sodium cacodylate, 15% (w/v) PEG 3400 (Aldrich), 100 mM ammonium acetate, and 50 mM sodium acetate (pH 4.6). The precipitant reservoir (1 mL) contained 30% (w/v) PEG 3400, 200 mM ammonium acetate, and 100 mM sodium acetate (pH 4.6). Crystals typically appeared within 7 days and grew to full size in 30 days.

Subtilisin 8397+1 was crystallized using the same method with the protein drop containing 2.5−5 mg/mL protein, 5 mM sodium cacodylate, 8.5% (w/v) PEG 3400, 8.5% (v/v) 2-propanol, and 50 mM sodium citrate (pH 5.6). The reservoir contained 17% (w/v) PEG 3400, 17% (v/v) 2-propanol, and 100 mM sodium citrate (pH 5.6). These crystals usually took 20 days to reach full size.

For data collection, large crystals of either 8397 (0.3 × 0.3 × 0.6 mm) or 8397+1 (0.2 × 0.3 × 0.7 mm) were transferred to thin-walled quartz capillary tubes (Charles Supper Co.). Crystals were dried and then mounted with the crystallization solution on either side of the crystal. The capillary tubes were sealed with sticky wax and mounted on a goniometer head for data collection.

Table 1. Data Collection and Data Reduction Statistics

	subtilisin 8397	subtilisin 8397+1
space group	$P2_1$	$P2_1$
unit cell dimnsns		
a (Å)	37.24	37.25 ± 0.02[a]
b (Å)	79.34	79.53 ± 0.04
c (Å)	41.51	41.56 ± 0.01
β (deg)	114.32	114.48 ± 0.04
no. of reflctns		
colld	11759	21228
obsd (>2σ)	7733	14501
resolution (Å)	2.2	1.8
no. of crystals	1	4
shells of data	3	4
R_{merge}[b] (%)		11.3

[a] Errors quoted are the standard deviation from the values measured for all crystals. [b] $R_{merge} = \sum|I_j - I_{ave}|\sum I_{ave}$, where j is a summation over all crystals.

Data Collection. X-ray data were measured to a nominal resolution of 2.2 Å for 8397 and 1.8 Å for 8397+1 using a four-circle diffractometer with a rotating anode X-ray source (AFC5R). Radiation was monochromatized using a graphite crystal. Individual background measurements were made for all reflections. Data from different crystals were merged together using a set of 265 common reflections which were measured for each crystal.[19] This common block of reflections was collected at the beginning and at the end of data collection. A radiation damage correction was applied as a function of both time and resolution using these reflections.[20] Programs for data reduction were written in the author's laboratory. Data collection results are summarized in Table 1.

Structure Refinement. The starting point for the refinement of both structures was the high-resolution structure of subtilisin 8350 reported by Pantoliano *et al.*[6] (PDB entry 1S01), stripped of all the water molecules and calcium ions. This structure was chosen as the starting model since 8397 was derived from 8350 by a single mutation (Lys 217 Tyr).[7] Both 8397 and 8397+1 were refined independently using XPLOR.[21,22]

Using XPLOR, simulated annealing was done in a single round. The 8350 structure was heated to 3000 K and cooled in increments of 25 K. After each cooling step, 50 steps of molecular dynamics simulation were performed. The time step for each of these runs was 0.5 fs. Conventional positional and *B*-factor refinement followed the simulated annealing refinement.

After the initial refinement of 8397, Lys 217 was changed to Ala in the model using the program O.[23] The same thing was done to Lys 217 and Lys 256 of 8397+1. After another round of refinement, Tyr side chains were modeled into the Ala positions using electron density difference Fourier maps ($2F_o - F_c$). In all three sites, there was reasonable density for the Tyr side chain at this point in refinement.

In both structures, it was observed that sufficient density for another atom existed beyond the sulfur of Cys 206 (Figure 1). Pantoliano *et al.*[6] also found extra density adjacent to the sulfur of Cys 206 in subtilisin 8350. They modeled this density as a second sulfur atom (cysteine persulfide, Cys−S−SH or Cys−S−S$^-$), an arrangement previously detected in the crystal structure of the sulfur-transfer protein rhodanese.[24] However, the size of the electron density in our structures was smaller and appeared to be due to a second-row element such as carbon, nitrogen, or oxygen. Cys−S−NH_2 is unknown in naturally

(16) Carter, P.; Wells, J. *Science* **1987**, *237*, 394−399.
(17) Jancarik, J.; Kim, S.-H. *J. Appl. Crystallogr.* **1991**, *24*, 409−411.
(18) Carter, C. W., Jr.; Carter, C. W. *J. Biol. Chem.* **1979**, *254*, 12219−12223.
(19) Monahan, J. E.; Schiffer, M.; Schiffer, J. P. *Acta Crystallogr.* **1967**, *22*, 322.
(20) Fletterick, R. J.; Sygusch, J.; Murray, N.; Madsen, N. B.; Johnson, L. N. *J. Mol. Biol.* **1976**, *103*, 1−13.
(21) Brünger, A. T.; Kuriyan, J.; Karplus, M. *Science* **1987**, *235*, 458−460.
(22) Brünger, A. *X-PLOR Version 3.1*; Yale University Press: New Haven, 1992; pp 75−77.
(23) Jones, T. A.; Zou, J. Y.; Cowan, S. W.; Kjeldgaard, M. *Acta Crystallogr.* **1991**, *A47*, 110−119.
(24) Ploegman, J. H.; Drent, G.; Kalk, K. H.; Hol, W. G. J. *J. Mol. Biol.* **1979**, *127*, 149−162.

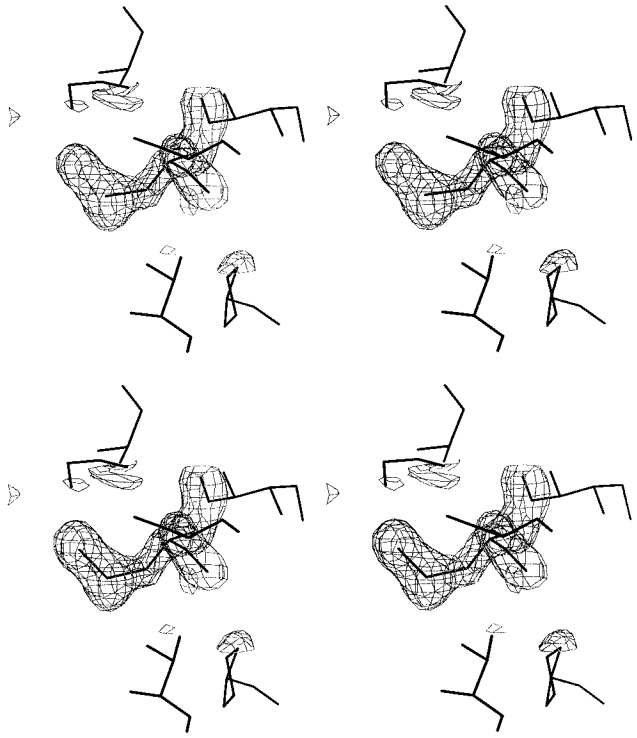

Figure 1. $2F_o - F_c$ electron density map for residue 206 of subtilisin 8397+1. Both maps are contoured at 1.2 σ. Panel A shows the density of residue 206 using F_c and phases derived from a model with the residue modeled as a cysteine. Panel B shows the density and coordinates for 206 after modeling the residue at cystenic acid (−S−OH). The added oxygen fits the extra density well. Similar results were seen with subtilisin 8397.

occurring enzymes,[25] and it is unclear how Cys−S−CH_3 would form in our structures. Cystenic acid (Cys−S−OH or Cys−S−O^-), on the other hand, has been proposed as an intermediate in the formation of sulfinic acid (Cys−SO_2H) and sulfonic acid (Cys−SO_3H).[26,27] Additionally, Syed *et al.*[28] has proposed a cystenic acid analog, Cys−Se−OH, as an intermediate during the oxidation of selenosubtilisin. Cystenic acid is a product of the active radical oxidation of cysteine.[26] We added OH to the model of Cys 206 at this point in the refinement. The ideal S−O bond length and angle were obtained from an average of all such bonds in the Cambridge Structural Database.[29] After subsequent refinement rounds, temperature factors for the extra oxygen did not rise above the average for overall side-chain atoms and the density was comparable to that of other side-chain oxygens.

Water molecules were located using $2F_o - F_c$ maps with a contour level of 1.2 σ. Electron density peaks sometimes appeared in the $2F_o - F_c$ maps as possible water molecules, but did not reappear in the same position or at all after water had been added to the structure. Only waters that reappeared after further refinement and had temperature factors less than 60 Å^2 were retained in the final model.

Initially, the calcium ions (Ca^{2+}) were modeled as water molecules. However, during intermediate steps of the refinement, the electron densities increased at these sites and the temperature factors decreased down to 2.0 Å^2, the lower limit set in XPLOR. These observations indicated that the cation site was occupied by something with more electrons than either a water or a sodium ion. These ions were modeled as calcium since this cation had been present during the purification steps while no additional potassium had been present. Our confidence in these calcium positions stemmed from the fact that calcium has been detected at these sites in structures reported previously.[9,12,30]

Figure 2. "Strong" calcium binding A site. For both panels, the density comes from a $2F_o - F_c$ map with F_c and phases derived from a model without Ca^{2+}. The contour level is 1.5 σ. Panel A shows calcium site A for 8397. The Ca^{2+} is coordinated with the carbonyl oxygens of Leu 75, Ile 79, and Val 81 and the side-chain oxygens of Gln 2, Asp 41, and Asn 77. Panel B shows the same calcium site for subtilisin 8397+1. The same coordination geometry for this tight calcium site is observed in both structures.

For 8397, a calcium ion was built into site A (Figure 2A). No density was observed for Ca^{2+} at the B site (Figure 3A). For 8397+1, calcium ions were built into sites A and B (Figures 2B and 3B). The refinement parameters used in XPLOR for the calcium ions have been deposited in the Protein Data Bank. During subsequent refinement rounds, the electron densities remained large and at 1.2 σ were continuous with several carbonyl oxygens (Figures 2 and 3B), again strengthening our confidence that these were calcium ions. A summary of the refinement results is in Table 2. Both of these structures have been deposited with the Protein Data Bank. Subtilisin 8397 has been assigned the code 1SBI, and subtilisin 8397+1 has been assigned the code 1SBH.

Discussion

Comparison of the 8397 and 8397+1 Structures. The backbone conformation of the proteins show no major differences between the two mutants. The root mean square (rms) deviation for the backbone atoms is 0.26 Å. The rms deviation for the side-chain atoms is 0.57 Å; however, some of the side chains do show significant rearrangements. Most of these rearrangements occur in surface side chains. Lys 43, Glu 156, Gln 185, and Tyr 217 all have significant changes.

The number of water molecules for 8397 and 8397+1 is 72 and 90, respectively. This difference is probably due to the differing resolutions of our structures. In both structures, we have been conservative in adding waters to the model. Other subtilisin structures solved at similar resolution (2.0−1.7 Å) report between 113 and 215 waters.[6,31−33]

Since the two mutants had been crystallized and data collected in different crystallization buffers (sodium acetate pH 4.6 for 8397 and sodium citrate pH 5.6 for 8397+1), we were concerned that differences in calcium binding may be due to differences

(25) Jocelyn, P. C. *Biochemistry of the SH Group*; Academic Press: New York, 1972; pp 14−46.
(26) Purdie, J. W. *J. Am. Chem. Soc.* **1967**, *89*, 226−230.
(27) Allison, W. S. *Acc. Chem. Res.* **1976**, *9*, 293−299.
(28) Syed, R.; Wu, Z.-P.; Hogle, J. M.; Hilvert, D. *Biochemistry* **1993**, *32*, 6157−6164.
(29) Allen, F. H.; Kennard, O.; Watson, D. G.; Brammer, L.; Orpen, A. G.; Taylor, R. *J. Chem. Soc., Perkin Trans. 2* **1987**, S1−S19.
(30) Bode, W.; Papamokos, E.; Musil, D. *Eur. J. Biochem.* **1987**, *166*, 673−692.
(31) Bott, R.; Ultsch, M.; Kossiakoff, A.; Graycar, T.; Katz, B.; Power, S. *J. Biol. Chem.* **1988**, *263*, 7895−7906.
(32) Erwin, C. R.; Barnett, B. L.; Oliver, J. D.; Sullivan, J. F. *Protein Eng.* **1990**, *4*, 87−97.
(33) Gallagher, T.; Bryan, P.; Gilliland, G. L. *Proteins*: *Str. Funct. Gen.* **1993**, *16*, 205−213.

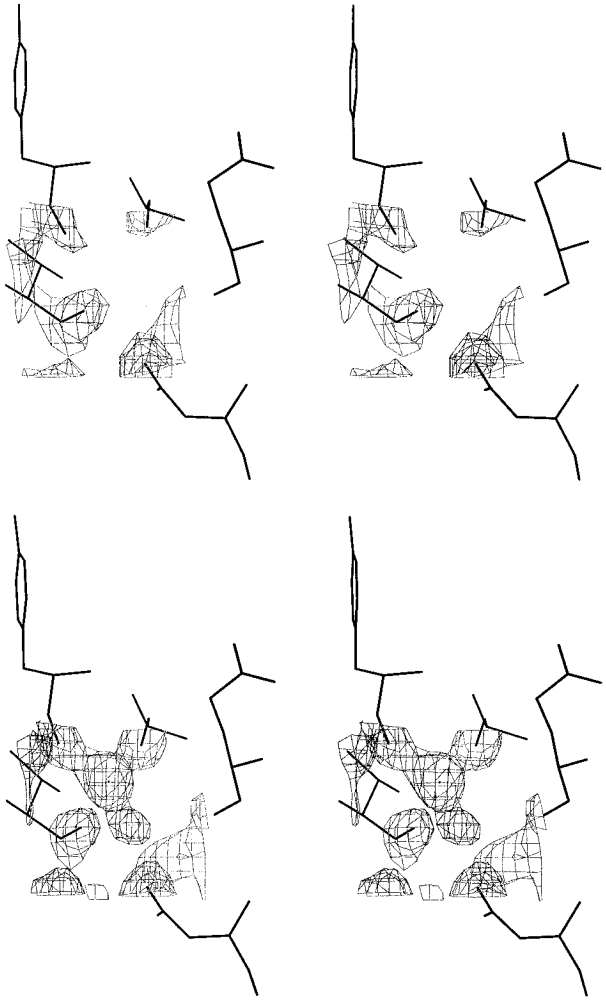

Figure 3. "Weak" calcium binding B site. For both panels, the density comes from a $2F_o - F_c$ map with F_c and phases derived from a model without Ca^{2+}. The contour level is 1.5 σ. (A) B site for 8397. There is no density within the site even down to a contour level of 0.8 σ. (B) B site for 8397+1. The calcium ion (shown as a dot in the figure) is associated with the carbonyl oxygens of Ala 169, Tyr 171, and Val 174. The Ca^{2+} is also closely associated with a water molecule (which is unmarked and is directly below the Ca^{2+} in the figure) which itself is associated with a side-chain oxygen of Asp 197 and the carbonyl oxygen of Glu 195.

in the pH of the crystallization solutions. To address this concern, we soaked crystals of 8397+1 in the same buffer and pH conditions that were used for 8397. The resulting structure shows that 8397+1 still binds two calcium ions at pH 4.6. It does not appear that the change in pH is related to the change in calcium ion binding.

Ramachandran plots[34] generated by PROCHECK[35] show only one residue, Ser 63, in the disallowed region in both structures. In both models, the Tyr 217 side chain strongly interacts with the Ser 63 side chain. The distance between the two side-chain hydroxyl oxygens is 2.67 Å in 8397 and 2.58 Å in 8397+1. It appears that these short hydrogen bonds allow Ser 63 to be in the disallowed region of the Ramachandran plot.

Oxidation State of Cys 206. The cysteine at position 206 is of special interest in both structures. While creating subtilisin 8350, Pantoliano *et al*. mutated both Gln 206 and Ala 216 to cysteines in order to increase stabilization through the introduction of a disulfide bond.[6,36] However, it was found experimentally that the single Gln 206 Cys mutation was more stable than the double mutation.[6] In their structure of the mutant, Pantoliano *et al*. modeled extra density beyond the SG as an extra sulfur atom. In both of our structures, we also observed extra density beyond SG (Figure 1A). However, since the density in our $2F_o - F_c$ maps did not appear large enough to be a sulfur atom, we modeled it as a hydroxyl. It should be noted that in our initial refinement model the residue at position 206 was cysteine and not cysteine persulfide, so the extra density past the sulfur of Cys 206 is not due to model bias. Figure 1B shows the density of 8397+1 at 206 after being modeled as cystenic acid and subsequent positional and *B*-factor refinement. The extra oxygen fits the density well. The electron density for Cys 206 in the 8397 structure was similar.

Table 2. Refinement Statistics[a]

	subtilisin 8397	subtilisin 8397+1
no. of water molecules	72	90
no. of calcium ions	1	2
R_{cryst} (%)	16.4	18.5
δ bond[b] (Å)	0.012	0.012
δ angle[b] (deg)	1.1785	1.694
overall *G*-factor[c]	better	better
mean *B*-factor (Å^2)		
main chain	13.4	18.9
side chain	14.3	21.7
overall protein	13.8	20.1
water	32.7	33.8
A site calcium	14.5	20.6
B site calcium		38.8

[a] The number of heavy atoms in the aqueous structures including the calciums is 1939 for 8397 and 1943 for 8397+1. For positional refinement, reflections with $F > 2.0\sigma(F)$ and within the resolution range 17−2.2 Å for 8397 and 17−1.8 Å for 8397+1 were used. For *B*-factor refinement, reflections with $F > 2.0\sigma(F)$ and within the resolution range 5−2.2 Å for 8397 and 5−1.8 Å for 8397+1 were included in calculations. The final *R*-factor was calculated using the 5−2.2 Å data shell for 8397 and the 5−1.8 Å data shell for 8397+1. [b] Root-mean-square discrepancies from ideal values. [c] The overall *G*-factor is derived from a comparison of the geometry of a structure to other structures in the Protein Data Bank solved at the same resolution. The calculation was done using the program PROCHECK.[35]

There are several instances where stable sulfenic acids are important in protein function.[27,37,38] However, such side chains are usually stabilized by the absence of adjacent thiols, hydrogen-bonding interactions, ionization to the sulfenate, and a nonpolar local environment.[38] The only one of these stabilizing features in subtilisin is the absence of neighboring thiols. In addition, it is somewhat surprising that the sulfenic acid did not undergo further oxidation to the sulfonic acid by the free radicals generated by the X-ray beam. Complete oxidation from the sulfenic acid to the sulfonic acid was observed in crystals of NADH peroxidase.[39]

One possible explanation to these problems is that some exogenous molecule containing a thiol has formed a disulfide with Cys 206 and that this extra molecule is partially disordered or not fully occupied in the crystal. At very low contour levels (0.8 σ in a $2F_o - F_c$ map), there is extra density extending beyond the oxygen of the sulfenic acid in both structures. The extra density is similar in both 8397 and 8397+1. Glutathione was modeled into this weak density, and the tripeptide fits the

(34) Ramakrishnan, C.; Ramachandran, G. N. *Biochem. J.* **1965**, *5*, 909−933.
(35) Laskowski, R. A.; MacArthur, M. W.; Moss, D. S.; Thornton, J. M. *J. Appl. Crystallogr.* **1993**, *26*, 283−291.
(36) Pantoliano, M. W.; Ladner, R. C.; Bryan, P. N.; Rollence, M. L.; Wood, J. F.; Poulos, T. L. *Biochemistry* **1987**, *26*, 2077−2082.
(37) Claiborne, A.; Miller, H.; Parsonage, D.; Ross, R. P. *FASEB J.* **1993**, *7*, 1483−1490.
(38) Claiborne, A.; Ross, R. P.; Parsonage, D. *Trends Biochem. Sci.* **1992**, *17*, 183−186.
(39) Stehle, T.; Ahmed, S. A.; Claiborne, A.; Schulz, G. E. *J. Mol. Biol.* **1991**, *221*, 1325−1344.

density reasonably well. A more complete understanding of the oxidation state of Cys 206 will require further experimentation.

Calcium Binding Sites. Subtilisin BPN′ binds two calcium ions.[6,30] One of these sites (site A) is close to the N-terminus and binds Ca^{2+} tightly ($K_d \approx 1 \times 10^{-8}$ M).[6] The second site (site B), some 32 Å away, binds Ca^{2+} much more weakly ($K_d \approx 32$ mM).[9] Calcium was not observed in this site in either the X-ray structure of subtilisin 8350 or the neutron structure of subtilisin BPN′.[6,10] By adding Ca^{2+} in the millimolar range, Matsubara *et al.*[40] showed that the rate of thermal inactivation decreases, which suggested that the occupation of the weak Ca^{2+} site is important for resisting thermal inactivation. Furthermore, mutants with enhanced affinity for the weaker Ca^{2+} site require less Ca^{2+} in order to resist thermal inactivation.[9]

The importance of calcium binding to thermostability is nicely illustrated by the thermophilic homologue of subtilisin, thermitase. Braxton and Wells[41] identified two sites of autoproteolysis, Ala 48-Ser 49 and Ser 163-Thr 164. Both of these sites are located in extended surface loops and are in regions of high mobility. In addition to the A and B sites, thermitase contains a third Ca^{2+} binding segment in the region surrounding the Ser 49 autocleavage site in subtilisin.[42] To improve the resistance to thermal-induced autolysis (and therefore inactivation), Braxton and Wells replaced the region around Ser 49 with the third thermitase Ca^{2+} binding sequence. This chimeric enzyme bound an extra Ca^{2+} with moderate affinity ($K_d \approx 100$ μM) and was slightly less stable to thermal inactivation in EDTA. However, in the presence of 10 mM $CaCl_2$, chimeric subtilisin was found to be 10-fold more stable to irreversible inactivation than wild-type subtilisin BPN′, thus illustrating the benefit of enhanced calcium binding to stability. In an analogous study, Toma *et al.*[43] have shown that introducing an extra calcium binding site from thermolysin into neutral protease improved by more than 2-fold the resistance of neutral protease to thermal inactivation.

In order to partially explain the increased stability seen for 8397+1 over 8397,[8] we first looked at the A and B calcium binding sites in both mutants. In both structures, the A site is similar to that observed previously for subtilisin BPN′,[9] subtilisin Carlsberg,[30] and thermitase.[42] As expected, a calcium ion is present in both structures. The coordination of the calcium in the A site can be thought of as a distorted octahedral arrangement with one bidendate ligand, Asp 41. The coordination geometry for both structures are shown in Figure 4A.

The A site consists primarily of a nine-residue surface loop next to the N-terminus. This loop interrupts the last turn of helix C, whose first turn contains the active site His 64. The major stabilizing effect of the A site is due to the calcium holding together helix C, the N-terminus, and the ω loop that includes Asp 41. Bryan and co-workers[33,44] have created several versions of subtilisin BPN′ that lack the A site through a deletion of residues 75−83 made in the context of several site-specific, stabilizing substitutions. When residues 75−83 of the A site are deleted, coupled with mutations near the N-terminus and in the ω loop generated by directed evolutionary techniques, the resulting mutant is 1000-fold more stable than native BPN′ in

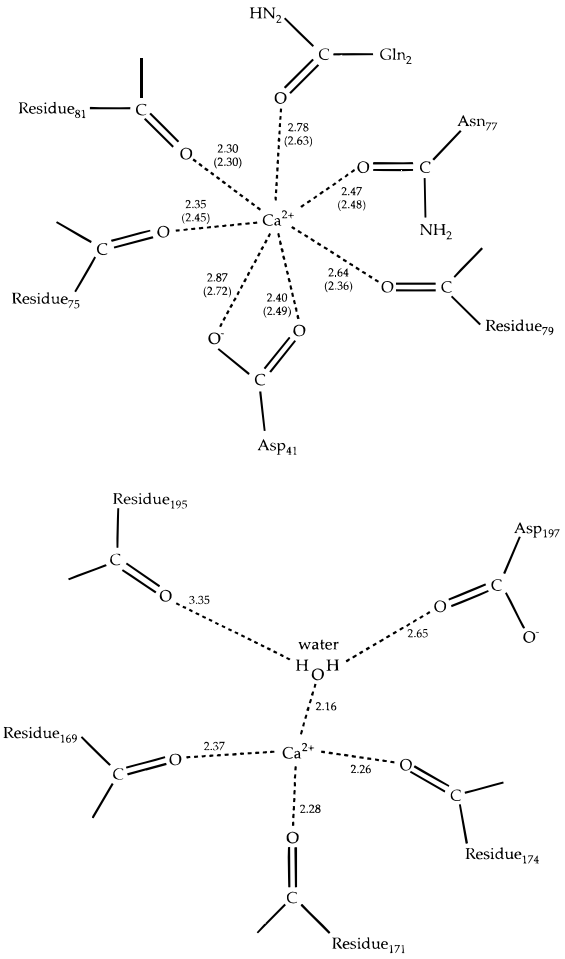

Figure 4. Cartoons of the calcium binding sites. (A) Calcium binding A site. Distances are indicated next to the dashed lines. The values in the parentheses are for subtilisin 8397. The other distances are for subtilisin 8397+1. (B) Calcium binding B site of 8397+1.

the presence of 10 mM EDTA at 65 °C. Their work demonstrates the numerous interactions and effects that the A site calcium has on native BPN′.

The B site in 8397 is unoccupied (Figure 3A), which was not unexpected since the binding constant for this site is 32 mM in subtilisin BPN′ and the mutations made to form 8397 were not designed to affect the B site. This site has been previously shown to be occupied in subtilisin BPN′ when $CaCl_2$ is present at 10 mM concentration.[9,32] In the absence of calcium, the B site of subtilisin BPN′ has previously been shown to be unoccupied in the crystal structure.[6] To our surprise, the B site is occupied in 8397+1 (Figure 3B), even though no additional $CaCl_2$ is present in the crystallization buffer. The site has a tetrahedral coordination geometry. One of the four calcium ligands is a water molecule; the other ligands are all backbone carbonyl oxygens. The water is also tightly bound to the side-chain oxygens of Asp 197. The presence of this water molecule prevents calcium from escaping into the solution. Figure 4B shows the distances for the chelating side chains. Except for the calcium and water in 8397+1, the protein atoms which make up the B sites in both 8397 and 8397+1 are very similar to each other.

Evidence for a weak calcium binding site was obtained by Pantoliano *et al.*[9] through the study of the effect of increasing calcium concentration on the kinetic thermal stability of wild-type subtilisin. They found that increasing the concentration of calcium above 0.10 mM up to 100 mM significantly decreases the rate of irreversible inactivation of BPN′ at 65 °C. Their

(40) Matsubara, H.; Hagihara, B.; Nakai, M.; Komaki, T.; Yonetani, T.; Okunuki, K. *J. Biochemistry* **1958**, *45*, 251−258.
(41) Braxton, S.; Wells, J. A. *Biochemistry* **1992**, *31*, 7796−7801.
(42) Gros, P.; Kalk, K. H.; Hol, W. G. J. *J. Biol. Chem.* **1991**, *266*, 2953−2961.
(43) Toma, S.; Campagnoli, S.; Margarit, I.; Gianna, R.; Grandi, G.; Bolognesi, M.; DeFilippis, V.; Fontana, A. *Biochemistry* **1991**, *30*, 97−106.
(44) Strausberg, S. L.; Alexander, P. A.; Gallagher, D. T.; Gilliland, G. L.; Barnett, B. L.; Bryan, P. N. *Bio/Technology* **1995**, *13*, 669−673.

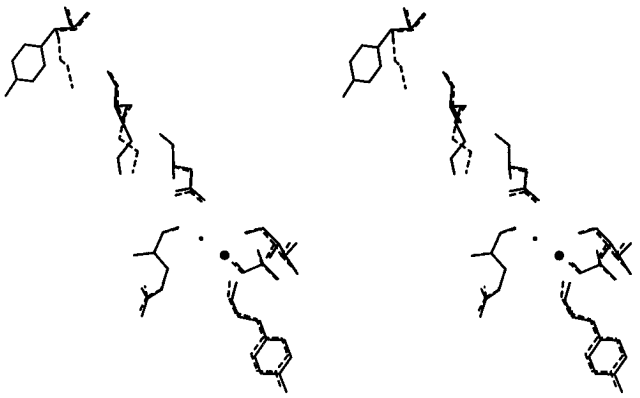

Figure 5. Stereoview of the superposition of key residues between surface residue 256 and the calcium binding B site. Subtilisin 8397+1 (solid lines) has a calcium ion (large sphere) and a water molecule (small sphere) present. Subtilisin 8397 residues are shown as dashed lines. The mutated residue is at the top of the figure, roughly 12 Å away from the B site. The end of the side chain has moved by ~6.5 Å. The second residue from the top is Lys 265 (also on the surface). It has moved ~1.06 Å away from the B site toward the carbonyl oxygen of Leu 196 (not shown).

data fit a theoretical titration curve for a binding site with an apparent $K_d \approx 32$ mM. The upper limit of attainable kinetic stability corresponds to a protein that binds 2 Ca^{2+}/mol of enzyme. Although 32 mM is a very weak binding constant, the only change observed in a crystal structure done at 40 mM Ca^{2+} involved binding at this site.[9]

In the absence of added calcium, the B site is known to bind a monovalent cation, such as sodium or potassium, when present as a counterion in the buffer of the crystallization solution.[9,11,41] We do have sodium (100 mM) present in our crystallization buffer; however, sodium is present for both 8397 and 8397+1. Density for a cation is only observed in the B site of the 8397+1 mutant. Moreover, the size of the electron density strongly suggests an ion from the third row.

Lysine 256 to Tyrosine Mutation. The only differences between 8397 and 8397+1 are the crystallization buffers and the single Lys 256 Tyr mutation. As pointed-out above, we have addressed the problem of dissimilar crystallization solutions and found that placing crystals of both mutants at the same pH did not alter the observed pattern of calcium binding. Therefore, the site of mutation must be important for altering the B site calcium binding affinity. Residue 256 is a surface residue approximately 12 Å away from the calcium binding B site (Figure 5). The side-chain hydroxyl of Tyr 256 in 8397+1 has moved roughly 6.5 Å away from the position of the side-chain nitrogen of Lys 256 in subtilisin 8397. The Tyr in 8397+1 is further from the B site than the Lys was in the 8397 structure. The tyrosine hydroxyl had displaced a water molecule (not shown) that is present in 8397. This water is hydrogen bonded to the carbonyl oxygen of Gly 258 at a distance of 3.30 Å. The distance between the hydroxyl of Tyr 256 and the carbonyl oxygen of Gly 258 is 3.35 Å.

Removing the side chain of Lys 256 in subtilisin 8397+1 causes the side chain of Lysine 265, another surface residue, to move ≈1 Å away from its position in 8397 (Figure 5). In the 8397+1 structure, the nitrogen of Lys 265 has moved away from Asp 197 (part of the B site) by 0.7 Å and toward the carbonyl oxygen of Leu 196 (not shown) by 0.5 Å. In 8397+1, the side chain of Asp 197 is too far from the Lys 265 side chain to form a strong interaction (4.02 Å in the 8397+1 structure, 3.32 Å in the 8397 structure). This lack of a stabilizing interaction allows Asp 197 to form a hydrogen bond to the water which locks the calcium into the B site in 8397+1.

It is interesting to note that Lys 265 is loosely associated with a densely packed side-chain cluster that is conserved among subtilisins. Heringa *et al.*[45] have identified eight possible clusters among seven subtilisins (subtilisin BPN′, subtilisin Carlsberg, mesentericopeptidase, thermitase, proteinase K, esperase, and savinase). The main features of these clusters is that the intracluster contacts dominate over those to their local environments and are positioned at strategic loop-connecting sites near the surface.[46] Lys 265 is associated with a strong cluster whose members include Ile 175, Arg 247, Gln 251, and Asp 197, part of calcium binding site B. The Asp cluster site is conserved among the seven subtilisin as either as Asp or a Glu. In general, these dense and isolated clusters may be strategic sites for protein folding and stability.[45]

Conclusion

This work shows that the overall structural changes induced by the Lys 256 Tyr mutation are minimal. The rms deviations between subtilisin 8397 and subtilisin 8397+1 are low, especially for the main-chain atoms. The binding of calcium to subtilisin 8397+1 has been enhanced even though the mutation occurred far from either calcium binding site. Even in the absence of calcium is the crystallization solution, both Ca^{2+} binding sites are occupied in 8397+1. In less stable subtilisin variants, only the high affinity A site is occupied.[6]

Our interest in mutating subtilisin was to create an enzyme that is more stable toward organic solvents, especially dimethylformamide. Sears *et al.*[8] created several variants derived from the thermostable subtilisin 8397.[5] Their approach was to remove surface charges one at a time: Lys 43 Asn, Lys 256 Tyr, and Asp 181 Asn. These residues were chosen for mutagenesis because of a lack of interaction with other nearby charged residues, and they were substituted with conserved uncharged residues found in other subtilisins. This approach has been successfully used for α-lytic protease.[47] In subtilisin, only the Lys 256 Tyr mutant exhibited enhanced thermostability. The crystal structure shows that this increase in stability was caused by a change in calcium binding rather than by removing a surface charge.

The work in this report shows that to fully understand the changes that have occurred to alter protein stability, it is essential to determine the structure of a protein—much like the need for a structure when analyzing mutations that alter enzyme function. The site of the Lys 256 Tyr mutation is ~12 Å away from the B site, yet it has altered the protein's ability to bind calcium and therefore its stability.

Acknowledgment. We thank Neela Yennawar and Kenneth Johnson for helpful discussions and much encouragement. This work was supported by the Office of Naval Research.

JA953443P

(45) Heringa, J.; Argos, P.; Egmond, M. R.; de Vlieg, J. *Prot. Eng.* **1995**, *8*, 21−30.
(46) Heringa, J.; Argos, P. *J. Mol. Biol.* **1991**, *220*, 151−171.
(47) Martinez, P.; Arnold, F. *J. Am. Chem. Soc.* **1991**, *113*, 6336−6337.